NUCLEAR SCIENCE AND TECHNIQUES **26**, 020402 (2015)

# Variance analysis for passive neutron multiplicity counting*

CHEN Li-Gao (陈利高),[1,2] GONG Jian (龚建),[1,†] WANG Kan (王侃),[2] XIE Qi-Lin (谢奇林),[1] LIU Xiao-Bo (刘晓波),[1] BAI Zhong-Xiong (白忠雄),[1] LU Yi (鲁艺),[1] RONG Ru (荣茹),[1] and YIN Yan-Peng (尹延朋)[1]

[1] *Institute of Nuclear Physics and Chemistry, China Academy of Engineering Physics, Mianyang 621900, China*
[2] *Department of Engineering Physics, Tsinghua University, Beijing 100084, China*

(Received June 26, 2014; accepted in revised form August 18, 2014; published online April 20, 2015)

Passive neutron multiplicity counting is widely used as a nondestructive assay technique to quantify mass of plutonium material. One goal of this technique is to achieve good precision in a short measurement time. In this paper, we describe a procedure to derive mass assay variance for multiplicity counting based on the three-parameter model, and analytical equations are established using the measured neutron multiplicity distribution. Monte Carlo simulations are performed to evaluate precision versus plutonium mass under a fixed measurement time with the equations. Experimental data of seven weapons-grade plutonium samples are presented to test the expected performance. This variance analysis has been used for the counter design and optimal gate-width setting at Institute of Nuclear Physics and Chemistry.

Keywords: Arms control and disarmament, Neutron multiplicity counting, Variance analysis, Plutonium, Neutron counting

DOI: 10.13538/j.1001-8042/nst.26.020402

## I. INTRODUCTION

The initial motivation of developing passive neutron multiplicity counting was accountability measurement of impure plutonium in safeguards. It collects the time-correlated neutrons emitted from plutonium to extract the mass information, which makes this technique as a nondestructive assay procedure. Neither the container nor the sample itself can shield the neutrons easily. This makes the technique extend to the field of arms control and disarmament [1–8], where there is a strong need of measuring the plutonium mass stored in sealed packages.

Compared with destructive assay or calorimetry for plutonium, neutron multiplicity counting is advantageous in that a measurement of less than 30 min can be of a good precision. After determining hardware performance of the counting system, low assay variance is the most important criterion. Both counter geometry arrangement and parameters setting in the assay model determine the assay variance. In addition, statistical error of each measurement should be obtained to evaluate the confidence of assay result. A method for estimating the expected assay variance for a sample of known mass, neutron multiplication, and ($\alpha$, n) reaction rate has been developed by ENSSLIN, which is known as Figure of Merit code [9]. However, to give the assay variance for unknown samples is important, too. In this paper, we report a physics-based variance analysis algorithm that needs no known parameters. Multiplicity equations of the three-parameter point model for plutonium assay are introduced first. Then, we describe detailed process to establish the analytical expressions for assay variance of multiplicity counting, using the measured neutron multiplicity distribution of unknown samples. Finally, performance of this approach is checked by Monte Carlo simulations and experimental data.

## II. THREE-PARAMETER POINT MODEL

For a typical plutonium sample, the unknown parameters include: (1) mass $m$, which is proportional to spontaneous fission rate $F$ of $^{240}$Pu; (2) neutron leakage multiplication $M$; and (3) ratio $\alpha$ of ($\alpha$, n) reaction neutrons to spontaneous fission neutrons. The neutron multiplicity equations of three-parameter point model provide a solution for the three unknowns [10]:

$$S = F\varepsilon M\nu_{s1}(1+\alpha), \tag{1}$$

$$D = \frac{f\varepsilon^2 f_d M^2}{2}\left[\nu_{s2} + \left(\frac{M-1}{\nu_{i1}-1}\right)\nu_{s1}(1+\alpha)\nu_{i2}\right], \tag{2}$$

$$T = \frac{F\varepsilon^3 f_t M^3}{6}\left\{\nu_{s3} + \left(\frac{M-1}{\nu_{i1}-1}\right)[3\nu_{s2}\nu_{i2} + \nu_{s1}(1+\alpha)\nu_{i3}] + 3\left(\frac{M-1}{\nu_{i1}-1}\right)^2 \nu_{s1}(1+\alpha)\nu_{i2}^2\right\}, \tag{3}$$

* Supported by the National Natural Science Foundation of China (No. 11375158), Science and Technology Development Foundation of CAEP (No. 2013B0103009)

† Corresponding author, gongjian@caep.cn

where, $\varepsilon$ is neutron detection efficiency; $f_{\rm d}$ is doubles gate fraction; $f_{\rm t}$ is triples gate fraction; $\nu_{\rm s1}$, $\nu_{\rm s2}$ and $\nu_{\rm s3}$ are three moments of spontaneous fission neutron distribution; $\nu_{\rm i1}$, $\nu_{\rm i2}$ and $\nu_{\rm i3}$ are three moments of induced fission neutron distribution; and $S$, $D$ and $T$, representing count rates of the singles, doubles and triples, respectively, are three moments of measured neutron multiplicity distribution.

## III. VARIANCE ANALYSIS MATHEMATICS

After a sample being placed and measured in detection chamber, the multiplicity shift register can record the foreground multiplicity distribution in the R+A gate and background distribution in the A gate. The first and second measured foreground moments, $f_1$ and $f_2$, and background moments $b_1$ and $b_2$ are

$$f_1=\sum_{i=1}^{\max}[ip(i)]=\sum_{i=1}^{\max}\left[i\frac{f(i)}{N_{\rm R+A}}\right], \tag{4}$$

$$f_2=\sum_{i=2}^{\max}[i(i-1)p(i)]=\sum_{i=2}^{\max}\left[i(i-1)\frac{f(i)}{N_{\rm R+A}}\right], \tag{5}$$

$$b_1=\sum_{i=1}^{\max}[ip(i)]=\sum_{i=1}^{\max}\left[i\frac{b(i)}{N_{\rm A}}\right], \tag{6}$$

$$b_2=\sum_{i=2}^{\max}[i(i-1)p(i)]=\sum_{i=2}^{\max}\left[i(i-1)\frac{b(i)}{N_{\rm A}}\right], \tag{7}$$

where, $f(i)$ and $b(i)$ are neutrons detected and counted in the gate interval after the predelay and long delay, respectively, following any signal-triggered measured events; $p(i)$ is probability for detecting $i$ neutrons; $N_{\rm R+A}=\sum\limits_{i=1}^{\max}f(i)$ and $N_{\rm A}=\sum\limits_{i=1}^{\max}b(i)$ are total triggers of foreground and background, respectively.

From Eqs. (4)– (7), one has the following standard deviation equations for $f_1$, $f_2$, $b_1$ and $b_2$

$$\sigma_{f_1}=\sqrt{\sum_{i=1}^{\max}\left[\frac{i}{N_{\rm R+A}}\sigma_{f(i)}\right]^2+\left[\sum_{i=1}^{\max}\left(-\frac{if(i)}{N_{\rm R+A}^2}\sigma_{N_{\rm R+A}}\right)\right]^2}, \tag{8}$$

$$\sigma_{f_2}=\sqrt{\sum_{i=2}^{\max}\left[\frac{i(i-1)}{N_{\rm R+A}}\sigma_{f(i)}\right]^2+\left[\sum_{i=2}^{\max}\left(-\frac{i(i-1)f(i)}{N_{\rm R+A}^2}\sigma_{N_{\rm R+A}}\right)\right]^2}, \tag{9}$$

$$\sigma_{b_1}=\sqrt{\sum_{i=1}^{\max}\left[\frac{i}{N_{\rm A}}\sigma_{b(i)}\right]^2+\left[\sum_{i=1}^{\max}\left(-\frac{ib(i)}{N_{\rm A}^2}\sigma_{N_{\rm A}}\right)\right]^2}, \tag{10}$$

$$\sigma_{b_2}=\sqrt{\sum_{i=2}^{\max}\left[\frac{i(i-1)}{N_{\rm A}}\sigma_{b(i)}\right]^2+\left[\sum_{i=2}^{\max}\left(-\frac{i(i-1)b(i)}{N_{\rm A}^2}\sigma_{N_{\rm A}}\right)\right]^2}, \tag{11}$$

where, $\sigma_{f(i)}=[f(i)]^{1/2}$, $\sigma_{b(i)}=[b(i)]^{1/2}$, $\sigma_{N_{\rm R+A}}=(N_{\rm R+A}^{1/2})$ and $\sigma_{N_{\rm A}}=(N_{\rm A})^{1/2}$, and Poisson-distribution is assumed for $f(i)$, $b(i)$, $N_{\rm R+A}$ and $N_{\rm A}$.

Doubles and Triples count rates are determined by moments of multiplicity distribution in the foreground R+A gate and background A gate as

$$D=S(f_1-b_1), \tag{12}$$

$$T=S[f_2-b_2-2b_1(f_1-b_1)]/2, \tag{13}$$

Using error transfer functions produce the following standard deviation equations for $\sigma_S$, $\sigma_D$ and $\sigma_T$

$$\sigma_S=\sqrt{S/t}, \tag{14}$$

$$\sigma_D=\sqrt{((f_1-b_1)\sigma_S)^2+(S\sigma_{f_1})^2+(-S\sigma_{b_1})^2}, \tag{15}$$

$$\sigma_T=\sqrt{\left(\frac{f_2-b_2-2b_1(f_1-b_1)}{2}\sigma_S\right)^2+\left(\frac{S}{2}\sigma_{f_2}\right)^2+\left(-\frac{S}{2}\sigma_{b_2}\right)^2+(-Sb_1\sigma_{f_1})^2+[S(-f_1+2b_1)\sigma_{b_1}]}, \tag{16}$$

For plutonium sample with impurities that yields neutrons from ($a$, n) reactions, a solution of $M$ is derived by eliminating $F$ and $a$ from the three-parameter model

$$a + bM + cM^2 + M^3 = 0, \tag{17}$$

where

$$a = \frac{-6T\nu_{s2}(\nu_{i1}-1)}{\varepsilon^2 f_t S(\nu_{s2}\nu_{i3}-\nu_{s3}\nu_{i2})},$$
$$b = \frac{2D[\nu_{s3}(\nu_{i1}-1)-3\nu_{s2}\nu_{i2}]}{\varepsilon f_d S(\nu_{s2}\nu_{i3}-\nu_{s3}\nu_{i2})},$$
$$c = \frac{6D\nu_{s2}\nu_{i2}}{\varepsilon f_d S(\nu_{s2}\nu_{i3}-\nu_{s3}\nu_{i2})} - 1$$

Eq. (17) is a function of just $S$, $D$ and $T$, so partial derivatives of $M$ with respect to $S$, $D$ and $T$ are given by

$$\frac{\partial M}{\partial S} = -\frac{\left(\frac{\partial a}{\partial S} + \frac{\partial b}{\partial S}M + \frac{\partial c}{\partial S}M^2\right)}{b + 2cM + 3M^2}, \tag{18}$$

$$\frac{\partial M}{\partial D} = -\frac{\left(\frac{\partial b}{\partial D}M + \frac{\partial c}{\partial D}M^2\right)}{b + 2cM + 3M^2}, \tag{19}$$

$$\frac{\partial M}{\partial T} = -\frac{\frac{\partial a}{\partial T}}{b + 2cM + 3M^2}, \tag{20}$$

where, $\partial a/\partial S = -a/S$, $\partial b/\partial S = -b/S$, $\partial c/\partial S = -(c+1)/S$, $\partial b/\partial D = b/D$, $\partial c/\partial D = (c+1)/D$, and $\partial a/\partial T = a/T$.

Standard deviation of $M$ is determined by

$$\sigma_M = \sqrt{\left(\frac{\partial M}{\partial S}\sigma_S\right)^2 + \left(\frac{\partial M}{\partial D}\sigma_D\right)^2 + \left(\frac{\partial M}{\partial T}\sigma_T\right)^2}, \tag{21}$$

After $M$ being determined, the final solution for $F$ based on the three-parameter model is:

$$F = \frac{\left[\frac{2D}{\varepsilon f_d} - \frac{M(M-1)\nu_{i2}S}{\nu_{i1}-1}\right]}{\varepsilon M^2 \nu_{s2}}, \tag{22}$$

Then partial derivatives of $F$ with respect to $S$, $D$ and $T$ are given by:

$$\frac{\partial F}{\partial S} = -\frac{M(M-1)\nu_{i2}}{\varepsilon M^2 \nu_{s2}(\nu_{i1}-1)}, \tag{23}$$

$$\frac{\partial F}{\partial D} = -\frac{2}{\varepsilon^2 f_d M^2 \nu_{s2}}, \tag{24}$$

$$\frac{\partial F}{\partial M} = -\frac{4D}{\varepsilon^2 f_d M^3 \nu_{s2}} - \frac{\nu_{i2}S}{\varepsilon M^2 \nu_{s2}(\nu_{i1}-1)}, \tag{25}$$

Standard deviation of $F$ is finally determined by:

$$\sigma_F = \sqrt{\left(\frac{\partial F}{\partial S}\sigma_S\right)^2 + \left(\frac{\partial F}{\partial D}\sigma_D\right)^2 + \left(\frac{\partial F}{\partial M}\sigma_M\right)^2}, \tag{26}$$

For all plutonium samples, whether or not they have ($\alpha$, n) reactions, relative standard deviation of mass can be finally expressed by:

$$\sigma_m = \sigma_F / F, \tag{27}$$

## IV. MONTE CARLO SIMULATION RESULTS

For testing the variance analysis procedure established in this work, Monte Carlo simulations were carried out on the new pile lab-neutron multiplicity counter (NPL-NMC) at Institute of Nuclear Physics and Chemistry, CAEP. As shown schematically in Fig. 1, it was built with a ring of $^3$He tubes (32 four-atm tubes specifically), embedded in moderator material (polyethylene) around the rectangular cavity, with tube spacing of 55 mm. The assay chamber is effectively 450 mm($l$) × 450 mm($w$) × 560 mm($h$). This geometry and the $^3$He tubes ensure an efficiency of about 12% and a die-away time of 60 μs.

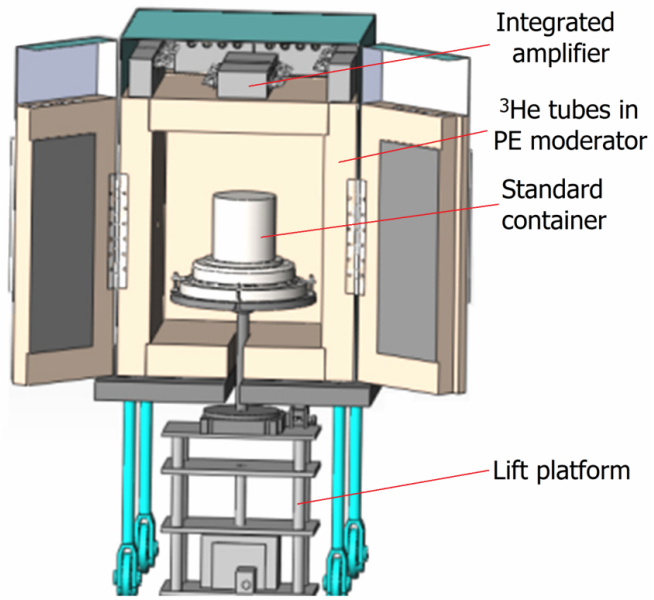


Fig. 1. (Color online) 3D view of the NPL-NMC.

The Monte Carlo code MCNPX, version 2.5.0 [11], which supports the spontaneous fission for plutonium and californium, was used in the simulation. A time stamped list of neutrons captured in $^3$He tubes was recorded, and processed by using a function for multiplicity shift register (MSR). In the simulation, dead-time effect was not introduced into the chain of time pluses. Thirty-two samples of pure metal plutonium of 20–4000 g, in isotopic composition of 5% $^{240}$Pu and 95% $^{239}$Pu, were placed in the center of NPL-NMC and simulated in a fixed counting time of 1000 s. Fig. 2 shows the assay mass relative standard deviation (RSD) from counting statistics versus the total mass of plutonium [12]. The multiplicity RSD for NPL-NMC decreases first, and then increases with plutonium mass. Physically speaking, at a low mass, RSD is dominated by precision of the number of correlated neutrons in the gate, which decreases with mass; while at a high mass, RSD is dominated by precision of the number of accidental neutrons in the gate, which increases with mass. The minimum RSD position is about 200 g under the parameters in the simulation.

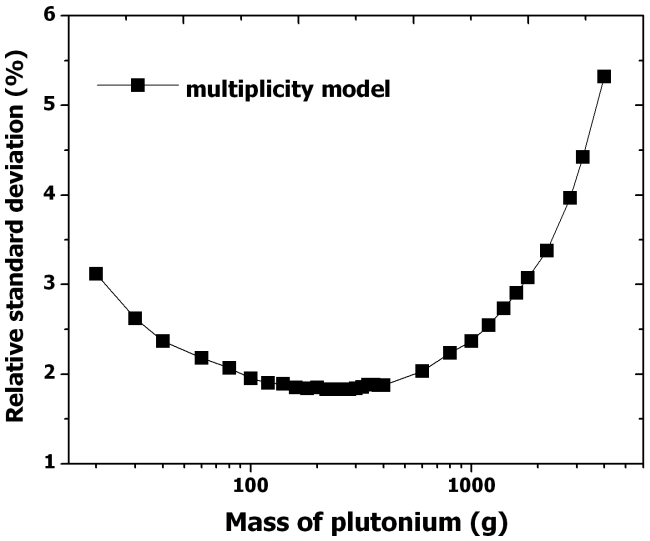


Fig. 2. Assay mass RSD(1 $\sigma$) *vs* total mass for pure plutonium metal sample within 1000 s count time for NPL-NMC, $Predelay$ = 3 μs, $Gate$=80 μs, $Longdelay$=4 ms.

TABLE 1. Plutonium compontes used for the experiment

| No. | Component shape | Nominal mass /g |
|---|---|---|
| $9\#^1$ | Hemispherical shell | 462 |
| $9\#^2$ | Hemispherical shell | 490 |
| $9\#^3$ | Hemispherical shell | 965 |
| $9\#^4$ | Hemispherical shell | 1 017 |
| $9\#^5$ | Spherical shell | 2 364 |
| $9\#^6$ | Hemispherical shell | 2 637 |
| $9\#^7$ | Hemispherical shell | 3 739 |

## V. EXPERIMENTAL RESULTS AND COMPARISONS

Measurements were done with seven weapons-grade plutonium components, which were sealed respectively in standard containers as shown schematically in Fig. 1 [13]. A set of integrated circuits on top of the counter were used to amplify the output signals of $^3$He tubes. One integrated circuit processing the input analog signals from four $^3$He tubes. A lift platform was used for position adjustment of the standard container. Each component was placed into the center of the detection chamber for a long period of time measurement, which was split up into a series of interval of 1000 s. Table 1 is the list of plutonium components used for the experiment.

For a given multiplicity counter, the counting precision resulting from MSR analysis depends mostly on the gate width setting. A gate of very short width shall compromise the precision because it misses signals and "sees" only a few coincidence events, while a gate of large width shall compromise the precision, because of the high level of random pile-up or accidental coincidence events [14], hence the importance of an optimum gate width to have the lowest RSD. Because the assay mass RSD is determined directly by the doubles and triples count rates, it is natural to calculate the minimum RSD position for these two count rates. The predelay was set to

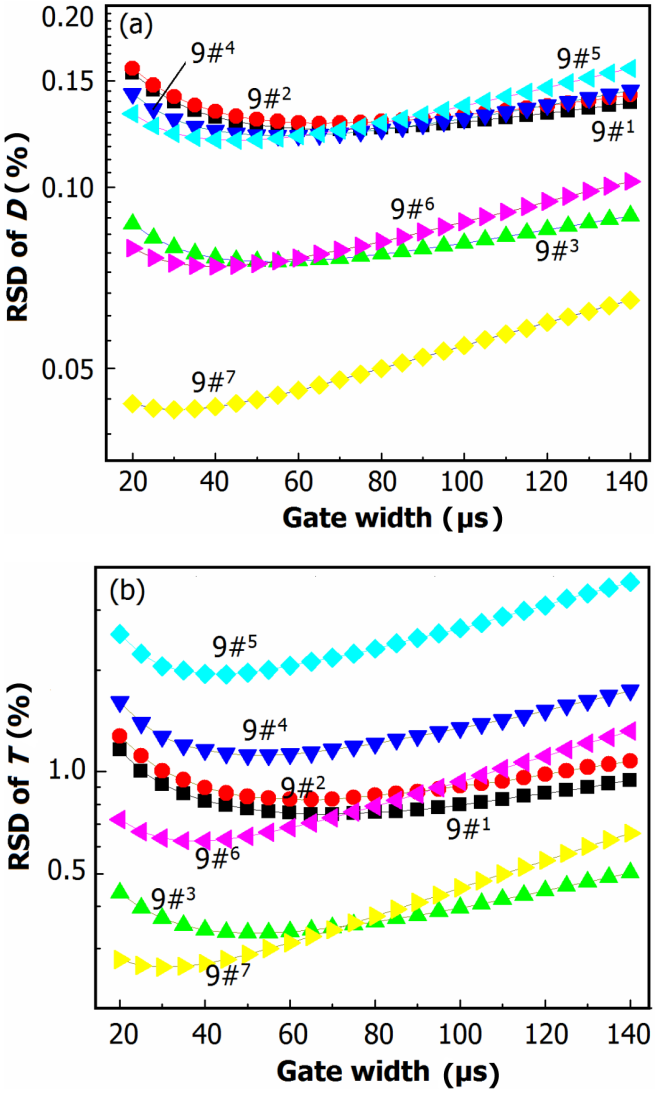


Fig. 3. (Color online) RSD(1 $\sigma$) of $D$ and $T$ *vs* gate width from seven samples of plutonium components.

9 μs to reduce the deadtime and pulses pileup effects based on speed of the integrated circuit. A measurement time of 3 hour was used for each sample. As shown in Fig. 3, the positions of minimum RSD are almost the same to doubles and triples count rate for each component, in the gate-width range of 30–90 μs. It means that the optimum gate-width setting has a broad option, which can be 0.5–1.5 times the die-away time. Finally, a gate of 60 μs is used for the NPL-NMC.

Because each measurement was split up into a number of 1000 s runs, the assay mass RSD can be acquired from the measured scatter of repeated runs based on the standard statistic theory, and the precision of the RSD is $(2n)^{-1/2}$, where $n$ is the number of runs [9]. The assay mass RSD can be calculated by the analysis model. The effect of counting dead time, coming from singal processing electronics, the RSD is not considered in the procedure described. However, from the RSD measurement results with coincidence circuits, we can be sure that the counting deadtime will not affect the RSD

TABLE 2. Comparison of measured and caculated assay mass RSD

| No. | $M$ | $n$[a] | RSD(1 $\sigma$)/% | | Bias/% | |
|---|---|---|---|---|---|---|
| | | | Measured | Cal. | RSD | Mass |
| $9\#^1$ | 1.154 | 23 | $2.46 \pm 0.36$ | 2.14 | 13 | 1.63 |
| $9\#^2$ | 1.140 | 18 | $2.15 \pm 0.36$ | 2.09 | 3 | 2.01 |
| $9\#^3$ | 1.446 | 56 | $1.85 \pm 0.17$ | 1.88 | 2 | 1.45 |
| $9\#^4$ | 1.153 | 23 | $2.56 \pm 0.38$ | 2.63 | 3 | 2.11 |
| $9\#^5$ | 1.189 | 25 | $3.28 \pm 0.46$ | 3.97 | 21 | 2.32 |
| $9\#^6$ | 1.497 | 60 | $1.86 \pm 0.17$ | 2.13 | 15 | 1.90 |
| $9\#^7$ | 2.098 | 22 | $1.97 \pm 0.30$ | 2.40 | 22 | 1.84 |

[a] $n$, number of 1000-second measurements.

greatly [15]. Background correction is not considered, either. Being just 3 counts/s, it results in a negligible error. Table 2 shows the comparison of measured and calculated RSD for the plutonium components.

## VI. CONCLUSION

An alternative procedure with analytical equations on the variance analysis has been estabilsihed based on the measured neutron multiplicity distribution without any prior knowledge of the sample. Simulation and experiment data show that it is possible to calculate assay variance with this approach. In a comparison of the measured and caculated RSDs, the maximum error is 22% while the minximum error is 2%. It is considered to be to a tolerable error for giving a referecnce confidence for the measured mass result. The most likely source of the error is the assumption that the foreground neutron multiplicity distribution is Poisson-distributed.

The approch descried in this paper has been used for the thermal passive multiplicity counter design and parameters setting in experimental assay at INPC. It also can be extended to other neutron counters, such as active multiplicity counter for uranium measurement, fast neutron multiplicity couner with scintillators.


[1] Ensslin N, Harker W C, Krick M S, *et al*. Application guide to neutron multiplicity counting. Los Alamos National Laboratory, LA-13422-M, 1998.

[2] Ye B, Zeng L N, Ying Y P, *et al*. Measurement of $k_{eff}$ with an improved neutron source multiplication method based on numerical analysis. Nucl Sci Tech, 2014, **25**: 020602. DOI: 10.13538/j.1001-8042/nst.25.020602

[3] Zhu L, Pu P and Han D D. Simulation of neutron diffusion and transient analysis of MSR. Nucl Sci Tech, 2014, **25**: 020601. DOI: 10.13538/j.1001-8042/nst.25.020601

[4] LI S P, XU X F, Cao H R, *et al*. Dynamic linear calibration method for a wide range neutron flux monitor system in ITER. Nucl Sci Tech, 2013, **24**: 040402.

[5] TUO X G, YANG J B, MU K L, *et al*. Monte Carlo simulation to key parameters of a compensated neutron logger. Nucl Sci Tech, 2009, **20**: 359–362.

[6] Geist W H, Mahmoud M R and Seo O S. IAEA neutron multiplicity measurements at the KAMS facility. the $51^{st}$ Annual Meeting of the Institute of Nuclear Materials Management, Baltimore, US, 2003.

[7] Macarthur D W, Whiteson R, Langner D, *et al*. Attribute measurement system with information barrier for the fissile material transparency technology demonstration system overview. Los Alamos National Laboratory, LA–UR–99–5611, 1999.

[8] Chambers D and David M. UK–Norway Initiative: Research into information barriers to allow warhead attribute verification without release of sensitive or proliferative information. the $51^{st}$ Annual Meeting of the Institute of Nuclear Materials Management, Baltimore, US, 2010.

[9] Ensslin N, Dytlewski N and Krick M S. Assay variance as a Figure-of-Merit for neutron multiplicity counting. Nucl Instrum Meth A, 1990, **A290**: 197–207.

[10] Cifarelli D M and Hage W. Models for a three parameter analysis of neutron signal correlation measurements for fissile material assay . Nucl Instrum Meth A, 1986, **A251**: 550–553.

[11] Pelowitz D B. MCNPX user's manual version 2.5.0. Los Alamos National Laboratory, LA-CP-05-0369, 2005.

[12] Chen L G, Liu X B, Gong J, *et al*. Neutron multiplicity stochastic simulation and parameters calculation research on big cavity detection system. High Power Laser Part Beams, 2014, **26**: 014005. (in Chinese) DOI: 10.3788/HPLPB201426.014005

[13] Chen L G, Liu X B, Gong J, *et al*. Neutron multiplicity counter design and calibration. J Tsinghua Univ: Nat Sci Ed, 2014, **54**: 159–163. (in Chinese)

[14] Stephen C, Louise G E and Melissa S. Optimal gate–width setting for passive neutron multiplicity counting. Los Alamos National Laboratory, LA-UR-10-04453, 2010.

[15] Carrillo L A, Ensslin N, Krick M S, *et al*. Uncertainty analysis for determination of plutonium mass by neutron multiplicity. Los Alamos National Laboratory, LA-UR-98-3044, 1998.